JOC Article

Design, Synthesis, and Evaluation of 9-D-Ribitylamino-1,3,7,9-tetrahydro-2,6,8-purinetriones Bearing Alkyl Phosphate and α,α-Difluorophosphonate Substituents as Inhibitors of Riboflavin Synthase and Lumazine Synthase

Mark Cushman,*,† Thota Sambaiah,† Guangyi Jin,† Boris Illarionov,‡ Markus Fischer,‡ and Adelbert Bacher‡

Department of Medicinal Chemistry and Molecular Pharmacology, School of Pharmacy and Pharmacal Sciences, Purdue University, West Lafayette, Indiana 47907, and Lehrstuhl für Organische Chemie und Biochemie, Technische Universität München, D-85747 Garching, Germany

cushman@pharmacy.purdue.edu

Received September 2, 2003

Lumazine synthase and riboflavin synthase catalyze the last two steps in the biosynthesis of riboflavin, an essential metabolite that is involved in electron transport processes. To obtain structural probes of these two enzymes, as well as inhibitors of potential value as antibiotics, a series of ribitylpurinetriones bearing alkyl phosphate and α,α-difluorophosphonate substituents were synthesized. Since the purinetrione ring system and the ribityl hydroxyl groups can be alkylated, the synthesis required the generation of these two moieties in protected form before the desired alkylation reaction could be carried out. These substances were designed as intermediate analogue inhibitors of lumazine synthase that would bind to its phosphate-binding site. All of the compounds were found to be effective inhibitors of both *Bacillus subtilis* lumazine synthase as well as *Escherichia coli* riboflavin synthase. Molecular modeling of the binding of 3-(1,3,7,9-tetrahydro-9-D-ribityl-2,6,8-trioxopurin-7-yl)propane 1-phosphate provided a structural explanation for how these compounds are able to effectively inhibit both enzymes. Interestingly, the enzyme kinetics of these new compounds in comparison with the parent purinetrione demonstrated unexpectedly that the phosphate and phosphonate substituents contributed negatively to the binding. A possible explanation for these effects on lumazine synthase would be that the inorganic phosphate in the assay buffer competes with the substituted purinetriones for binding to the enzyme. This would be consistent with the observed increase in K_m of the 3,4-dihydroxybutanone-4-phosphate substrate from 5.2 μM in Tris buffer or from 6.7 μM in MOPS buffer to 50 μM in phosphate buffer when tested on *Bacillus subtilis* lumazine synthase. However, when tested in Tris buffer vs *Mycobacterium tuberculosis* lumazine synthase, three of the phosphate inhibitors displayed inhibition constants in the 4−5 nM range, indicating that they are much more potent than the parent purinetrione. Under these conditions, the phosphate moieties of the inhibitors do contribute positively to their binding. The α,α-difluorophosphonate analogue, which is expected to have enhanced metabolic stability relative to the phosphates, was also found to be an inhibitor of *Mycobacterium tuberculosis* lumazine synthase with a K_i of 60 nM.

Introduction

The riboflavin synthase-catalyzed dismutation of two molecules of 6,7-dimethyl-8-D-ribityllumazine (**3**) (Scheme 1) results in the formation of one molecule of riboflavin (**4**) and one molecule of the substituted pyrimidinedione (**1**). In a wonderful example of efficient recycling catalyzed by lumazine synthase, the product **1** of the riboflavin synthase-catalyzed reaction is condensed with the four-carbon phosphate **2** to form the riboflavin synthase substrate **3**.[1−5]

Although the intricate details remain to be established, the lumazine synthase-catalyzed reaction most likely proceeds along the mechanistic pathway outlined in Scheme 2.[6] Condensation of the primary amino group of the substituted pyrimidinedione **1** with the ketone **2** is proposed to result in the formation of a Schiff base **5**,

* To whom correspondence should be addressed. Tel: 765-494-1465. Fax: 765-494-6790.
† Purdue University.
‡ Technische Universität München.

(1) Plaut, G. W. E.; Smith, C. M.; Alworth, W. L. *Annu. Rev. Biochem.* **1974**, *43*, 899−922.
(2) Plaut, G. W. E. In *Comprehensive Biochemistry*; Florkin, M., Stotz, E. H., Eds.; Elsevier: Amsterdam, 1971; Vol. 21, pp 11−45.
(3) Beach, R. L.; Plaut, G. W. E. *J. Am. Chem. Soc.* **1970**, *92*, 2913−2916.
(4) Bacher, A.; Eberhardt, S.; Richter, G. In *Escherichia coli and Salmonella: Cellular and Molecular Biology*, 2nd ed.; Neidhardt, F. C., Ed.; ASM Press: Washington, DC, 1996; pp 657−664.
(5) Bacher, A.; Fischer, M.; Kis, K.; Kugelbrey, K.; Mörtl, S.; Scheuring, J.; Weinkauf, S.; Eberhardt, S.; Schmidt-Bäse, K.; Huber, R.; Ritsert, K.; Cushman, M.; Ladenstein, R. *Biochem. Soc. Trans.* **1996**, *24*, 89−94.
(6) Volk, R.; Bacher, A. *J. Am. Chem. Soc.* **1988**, *110*, 3651−3653.

10.1021/jo030278k CCC: $27.50
Published on Web 01/03/2004

SCHEME 1

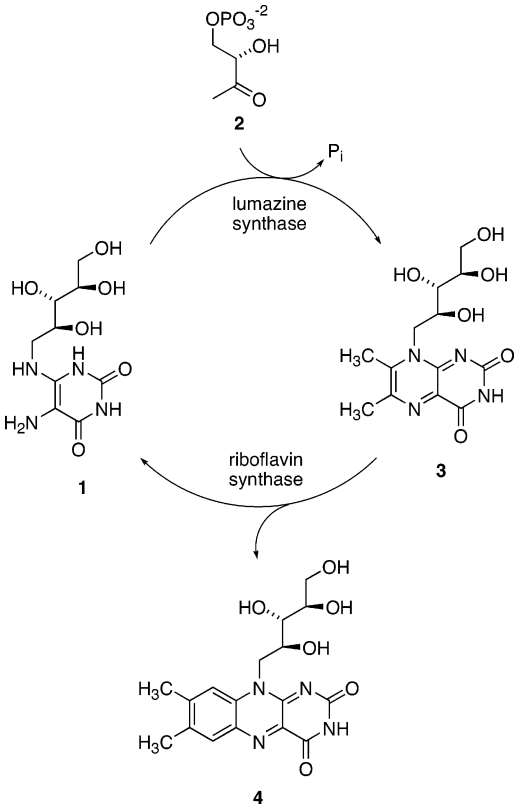

which eliminates phosphate to yield the enol **6**. Tautomerization of the enol **6** to the ketone **7**, ring closure, and dehydration of the covalent hydrate **8** would provide the product **3**.

X-ray crystallography of a complex of the phosphonate analogue **9**[7] with lumazine synthase has established that the phosphate of the hypothetical Schiff base binds far away from the ribityl side chain as depicted roughly in structure **5**.[8] As shown in Figure 1, the observed conformation of the phosphonate side chain of **9** implies that the phosphate of **5** would be stabilized by hydrogen bonding to the Arg136 residue and to the neighboring Thr95 (not shown). However, the details of the isomerization of the trans Schiff base to a cis Schiff base, or possible initial formation of a thermodynamically less stable cis Schiff base, have not been established. In addition, the timing of the phosphate release relative to the conformational change of the side chain to form **7** is still an open question. For example, a case has recently been made for the movement of the whole phosphate side chain of **5** toward a cyclic conformation before phosphate elimination occurs.[9]

The purinetrione **10** was recently synthesized as part of a program to obtain lumazine synthase inhibitors that might have value as structural probes of the active site of lumazine synthase.[10] Compound **10** acted as a partial

SCHEME 2

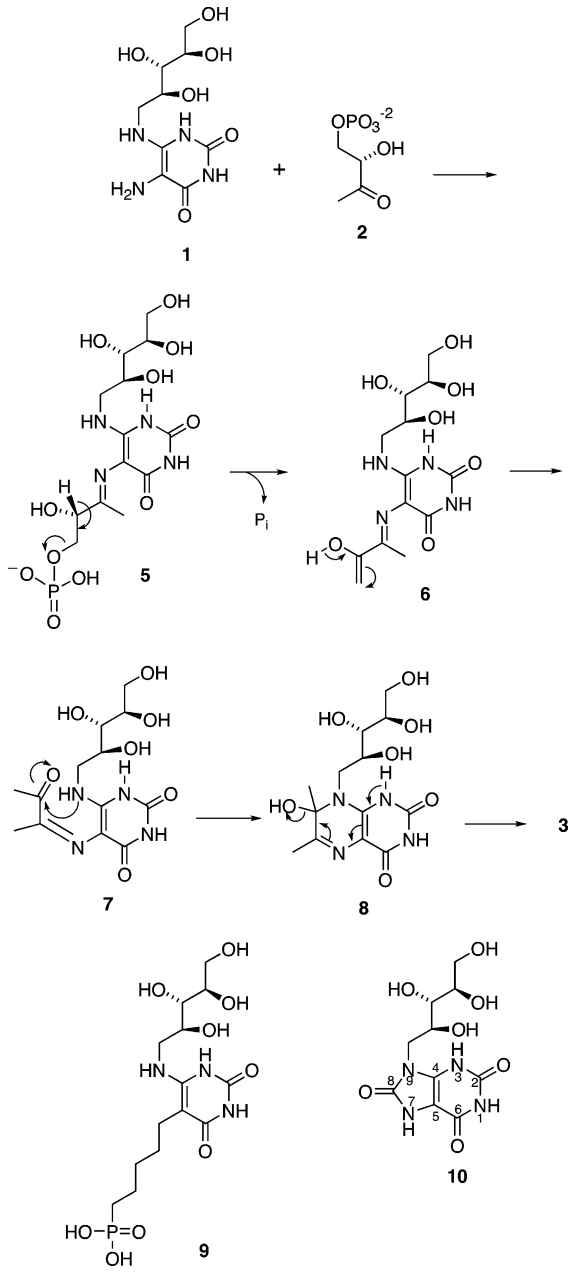

inhibitor of *Bacillus subtilis* lumazine synthase and displayed a K_i of 46 μM. In addition, it was a competitive inhibitor of *Escherichia coli* riboflavin synthase with a K_i of 0.61 μM. These K_i values indicated that the purinetrione **10** was among the most potent inhibitors of these two enzymes.[10] The present research project was undertaken to test the hypothesis that the attachment of alkyl phosphate side chains to the N-7 nitrogen of the purinetrione **10** would position the phosphate near the phosphate-binding site of the enzyme and thus result in an increase in potency for inhibition of lumazine synthase. Since the exact linker chain length that would be most favorable was an open question, a homologous series of four phosphates were planned in which the linker length was varied from three to six carbons. The resulting inhibitors might also be of potential therapeutic value as antibiotics because certain Gram-negative pathogenic bacteria and yeasts lack an efficient riboflavin uptake

(7) Cushman, M.; Mihalic, J. T.; Kis, K.; Bacher, A. *J. Org. Chem.* **1999**, *64*, 3838−3845.
(8) Meining, W.; Mörtl, S.; Fischer, M.; Cushman, M.; Bacher, A.; Ladenstein, R. *J. Mol. Biol.* **2000**, *299*, 181−197.
(9) Zhang, X.; Meining, W.; Cushman, M.; Haase, I.; Fischer, M.; Bacher, A.; Ladenstein, R. *J. Mol. Biol.* **2003**, *328*, 167−182.
(10) Cushman, M.; Yang, D.; Kis, K.; Bacher, A. *J. Org. Chem.* **2001**, *66*, 8320−8327.

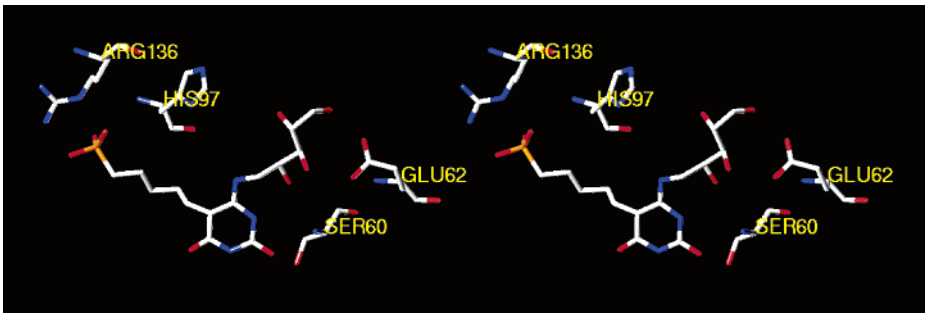

FIGURE 1. Crystal structure of phosphonate **9** bound in the active site of *Saccharomyces cerevisiae* riboflavin synthase. The figure is programmed for walleyed viewing.

system and are therefore absolutely dependent on endogenous riboflavin biosynthesis.[11−14]

Results and Discussion

Since the ribityl hydroxyl groups and the pyrimidinedione ring of **10** have the potential to be alkylated, the instillation of alkyl phosphate side chains on N-7 of the purinetrione system **10** requires that the ribityl substituent and the pyrimidinedione ring be generated in protected forms. Consequently, commercially available 6-chloro-2,4-dimethoxypyrimidine (**11**) was chosen as the starting material (Scheme 3). Our plan was to carry the dimethoxypyrimidine moiety through to a relatively late stage in the synthesis and then unmask the pyrimidinedione system under acidic conditions. This strategy would also allow the instillation and removal of *tert*-butyldimethylsilyl protecting groups for the alcohols.

Nitration of the starting material was performed as described in the literature with a mixture of fuming nitric acid and sulfuric acid to afford the nitrated intermediate **12**.[15] A nucleophilic aromatic substitution reaction with ribitylamine yielded the expected product **13**. The four ribityl hydroxyl groups were then protected as their *tert*-butyldimethylsilyl ethers to provide compound **14**. The pyrimidine system was converted to the substituted purine **15** through catalytic reduction of the nitro group to the corresponding amine over palladium on carbon. Reaction of the resulting primary amine with ethyl chloroformate, followed by heating the intermediate ethyl carbamate with sodium ethoxide in refluxing ethanol, provided the protected purine system **15**. Reaction of **15** with 1,4-diiodobutane, 1,5-diiodopentane, and 1,6-diiodohexane in DMF, with K_2CO_3 as the base, provided the corresponding monoalkylated products **16**, **17**, and **18** in good yields. Nucleophilic displacement reactions of the three iodides with silver dibenzyl phosphate resulted in the phosphates **20**, **21**, and **22**, having linker chain lengths of four, five, and six carbons.

The dibenzyl phosphate **19**, having a linker chain length of three carbons, was obtained during the exploration of a slightly different route outlined in Scheme 4. This route is simply a reversal in the sequence of steps and involves nucleophilic displacement of one of the iodides of 1,3-diiodopropane with silver dibenzyl phosphate, followed by the displacement of the second iodide with intermediate **15** as the nucleophile to afford **19**. This route was not tried out of necessity because the other sequence failed. It was simply tried in order to see if the reversed sequence of steps would work.

Selective deprotection of the ribityl side chains of **19**−**22** with hydrogen fluoride−pyridine in THF afforded the four tetraols **23**−**26**.[16−20] Interestingly, the potential conversion of the secondary alcohols to alkyl fluorides, which is reported to occur with hydrogen fluoride-pyridine in *n*-hexane, was not observed in the present case.[21] Cleavage of the two methyl groups and the two benzyl groups in the penultimate intermediates **23**−**26** with HCl in refluxing methanol afforded the four desired target compounds **27**−**30**.

Although the four phosphates **27**−**30** are interesting as potential lumazine synthase and riboflavin synthase inhibitors and as structural probes of the active sites of these enzymes, their potential use as antibiotics could be limited by the fact that phosphates are in general readily hydrolyzed by phosphatases. One approach to overcome this problem would be to replace the phosphate group in these compounds with an analogue that mimics the steric and electronic character of a phosphate, but is metabolically more stable. An α,α-difluorophosphonate seems like a good choice in the present case, since it would more closely mimic the acidity of a phosphate than a simple unfluorinated phosphonate would.[22,23] To test whether the enzyme inhibitory activity would be retained as a result of this replacement, the α,α-difluorophosphonate analogue of the least active riboflavin synthase inhibitor **28** was synthesized. The starting material **33** (Scheme 5) was prepared as described in the literature by reaction of the anion derived from diethyl difluoromethanephosphonate with 1,4-diiodobutane.[24] Reaction of the protected purinetrione **15** with the iodide **33** in the

(11) Wang, A. *Yichuan Xuebao* **1992**, *19*, 362−368.
(12) Oltmanns, O.; Lingens, F. *Z. Naturforsch.* **1967**, *22*, 751−754.
(13) Logvinenko, E. M.; Shavlovsky, G. M. *Mikrobiologiya* **1967**, *41*, 978−979.
(14) Neuberger, G.; Bacher, A. *Biochem. Biophys. Res. Commun.* **1985**, *127*, 175−181.
(15) Nutiu, R.; Boulton, A. J. *J. Chem. Soc., Perkin Trans. 1* **1976**, 1327−1331.
(16) Kendall, P. M.; Johnson, J. V.; Cook, C. E. *J. Org. Chem.* **1979**, *44*, 1421−1424.
(17) Newton, R. F.; Reynolds, D. P.; Webb, C. F.; Roberts, S. M. *J. Chem. Soc., Perkin Trans. 1* **1981**, 2055−2058.
(18) Ogawa, Y.; Nunomoto, M.; Shibasaki, M. *J. Org. Chem.* **1986**, *51*, 1625−1627.
(19) Snider, B. B.; Shi, Z. *J. Am. Chem. Soc.* **1994**, *116*, 549−557.
(20) Merino, P.; Franco, S.; Merchan, F. L.; Tejero, T. *Tetrahedron Lett.* **1998**, *39*, 6411−6414.
(21) Olah, G. A.; Nojima, M.; Kerekes, I. *Synthesis* **1973**, 786−787.
(22) Kabachnik, M. I.; Mastrukova, T. A.; Shipov, A. E.; Melentyeva, T. A. *Tetrahedron* **1960**, *9*, 10−28.
(23) Smyth, M. S.; Ford, H., Jr.; Burke, T. R., Jr. *Tetrahedron Lett.* **1992**, *33*, 4137−4140.

SCHEME 3[a]

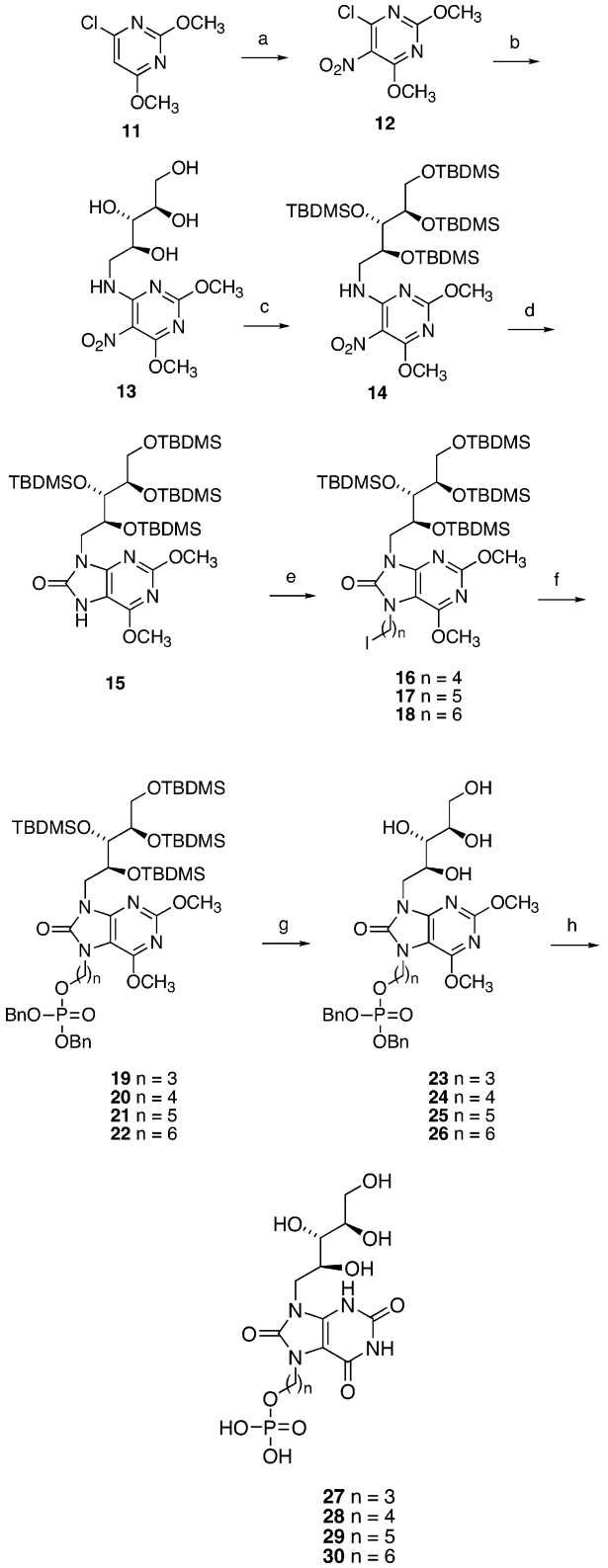

[a] Reagents and conditions: (a) fuming HNO_3, H_2SO_4, 80−85 °C (2.5 h); (b) ribitylamine, DMF, 23 °C (48 h); (c) TBDMSCl, imidazole, 23 °C (2 days); (d) (1) H_2, Pd/C, MeOH, 23 °C (3 days), (2) EtOCOCl, Et_3N, CH_2Cl_2, 0 °C (6 h), (3) NaOEt, EtOH, reflux (24 h); (e) diiodoalkane, K_2CO_3, DMF, 23 °C (24 h); (f) $AgOPO(OBn)_2$, CH_3CN, reflux (12 h); (g) HF−Py, THF, 0−23 °C (19 h); (h) HCl, MeOH, reflux (3 h).

SCHEME 4[a]

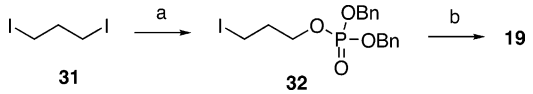

[a] Reagents and conditions: (a) $AgOPO(OBn)_2$, CH_3CN, reflux (10 h); (b) **15**, K_2CO_3, DMF, 23 °C (24 h).

SCHEME 5[a]

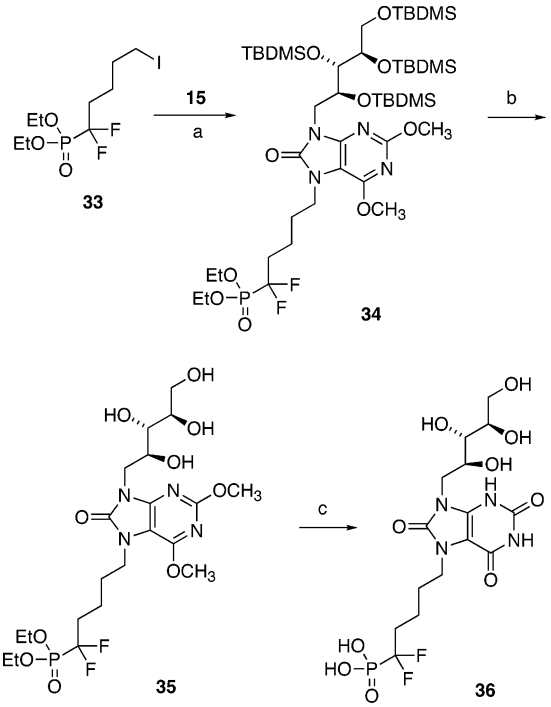

[a] Reagents and conditions: (a) K_2CO_3, DMF, 23 °C (24 h); (b) HF−Py, THF, 0−23 °C (19 h); (c) TMSI, CH_2Cl_2, 23 °C (24 h).

presence of potassium carbonate in DMF afforded the alkylation product **34**. The TBDMS groups were removed from **34** with hydrogen fluoride-pyridine in THF, resulting in intermediate **35**. Finally, the methyl ethers and ethyl esters were cleaved in the presence of trimethylsilyl iodide to yield the desired α,α-difluorophosphonate analogue **36**. This transformation proceeded in higher overall yield than the conversions of **23**−**26** to **27**−**30** with HCl−MeOH. However, when TMSI was tried for the conversions of **23**−**26** to **27**−**30**, the undesired cleavage of the phosphate groups to the corresponding alkyl iodides was observed.

The phosphates **27**−**30**, as well as the α,α-difluorophosphonate analogue **36**, were tested as inhibitors of recombinant *B. subtilis* lumazine synthase β_{60} capsids and recombinant riboflavin synthase from *E. coli*. The inhibition constants and types of inhibition displayed by these compounds are listed in Table 1, along with the previously published results of the structurally related phosphonates **37**−**40** and **9**, the phosphate **41**, and the purinetrione **10**. The new phosphates **27**−**30** and the α,α-difluorophosphonate **36** are reaction intermediate analogues that contain structural elements corresponding to both of the substrates **1** and **2**. Consequently, these

(24) Halazy, S.; Ehrhard, A.; Danzin, C. *J. Am. Chem. Soc.* **1991**, *113*, 315−317.

TABLE 1. Inhibition Constants vs *Bacillus subtilis* Lumazine Synthase and *Escherichia coli* Riboflavin Synthase

		lumazine synthase[a] K_i (μM)		
compd	parameter	variable **1** concn[c]	variable **2** concn[d]	riboflavin synthase[b] K_i (μM)
27	K_s[e]	3.82 ± 0.403	39.6 ± 4.24	1.94 ± 0.270
	k_{cat}[f]	2.26 ± 0.113	3.62 ± 0.145	16.66 ± 0.487
	K_i[g]	41.4 ± 18.1		3.63 ± 0.431
	K_{is}[h]	98.3 ± 45.8	211 ± 18.0	
	k_{cat}'	1.15 ± 0.265		
		mechanism: partial inhibition	mechanism: uncompetitive inhibition	mechanism: competitive inhibition
28	K_s	3.18 ± 0.397	25.7 ± 1.57	2.09 ± 0.222
	k_{cat}	3.13 ± 0.101	5.38 ± 0.111	16.67 ± 0.357
	K_i	168 ± 25.6		332 ± 83.0
	K_{is}		852 ± 103	
		mechanism: competitive inhibition	mechanism: uncompetitive inhibition	mechanism: competitive inhibition
29	K_s	3.82 ± 0.403	40.0 ± 3.92	1.96 ± 0.214
	k_{cat}	3.05 ± 0.094	3.65 ± 0.131	16.67 ± 0.387
	K_i	271 ± 84.6	852 ± 388	2.44 ± 0.230
	K_{is}	653 ± 163	817 ± 212	
		mechanism: mixed inhibition	mechanism: mixed inhibition	mechanism: competitive inhibition
30	K_s	3.00 ± 0.496	34.7 ± 4.00	2.26 ± 0.267
	k_{cat}	1.88 ± 0.081	3.85 ± 0.153	17.3 ± 0.462
	K_i	78.3 ± 20.4	175 ± 25.3	17.3 ± 1.72
	K_{is}	518 ± 178		
		mechanism: mixed inhibition	mechanism: competitive inhibition	mechanism: competitive inhibition
36	K_s	3.7 ± 0.78		2.13 ± 0.257
	k_{cat}	2.7 ± 0.092		12.53 ± 0.304
	K_i	132 ± 45		39.36 ± 9.91
	K_{is}	543 ± 169		
	k_{cat}'	1.1 ± 0.22		
		mechanism: partial inhibition		mechanism: competitive inhibition
37	K_i		440 ± 200	>1000
	K_{is}		640 ± 300	
			mechanism: mixed inhibition	
9	K_i		180 ± 88	>1000
	K_{is}		350 ± 22	
			mechanism: mixed inhibition	
38	K_i		130 ± 33	>1000
	K_{is}		140 ± 15	
			mechanism: mixed inhibition	
10	K_s			9.6 ± 0.9
	K_i		46 ± 5	0.61 ± 0.05
	K_{is}		250 ± 42	
	k_{cat}			39.9 ± 0.7
			mechanism: partial inhibition	mechanism: competitive inhibition
39	K_s			7.7 ± 2.3
	K_i		> 860	160 ± 87
	K_{is}			390 ± 63
				mechanism: mixed inhibition
40	K_s		>1000	6.8 ± 2.0
	K_i			170 ± 79
	K_{is}			590 ± 90
				mechanism: mixed inhibition
41	K_s		33 ± 3.2	5.7 ± 0.9
	K_i		830 ± 170	190 ± 39
	K_{is}		2000 ± 360	8200 ± 3200
				mechanism: mixed inhibition

[a] Recombinant β_{60} capsids from *B. subtilis*. [b] Recombinant riboflavin synthase from *E. coli*. [c] The concentration of the dihydroxybutanone phosphate substrate **2** was held constant at 100 μM during the assay, while the concentration of the pyrimidinedione substrate **1** was varied. [d] The concentration of the pyrimidinedione substrate **1** was held constant at 170 μM during the assay, while the concentration of the dihydroxybutanone phosphate **2** was varied. [e] K_s is the substrate dissociation constant for the equilibrium E + S → P. [f] k_{cat} is the rate constant for the process ES → E + P. [g] K_i is the inhibitor dissociation constant for the process E + I → EI. [h] K_{is} is the inhibitor dissociation constant for the process ES + I → ESI.

compounds can be classified as "bisubstrate analogue inhibitors" of lumazine synthase that could potentially achieve increased potency through an entropic advantage resulting from the linking of structural moieties that mimic each substrate. Since these compounds can potentially inhibit the binding of both substrates to lumazine synthase, it is possible that apparent differences in the inhibition mechanism and the inhibition constants could result from which substrate concentration is varied and which is held constant during the course of the enzyme inhibition experiments. To explore this question in more detail, two sets of inhibition experiments were conducted with lumazine synthase, one with variable pyrimidinedione **1** concentration and one with variable dihydroxybutanone phosphate **2** concentration. The results listed in Table 1 document an apparent change in inhibitory mechanism from partial inhibition with **27**, or from competitive inhibition with **28**, to uncompetitive inhibition as the substrate with the variable substrate concentration is switched from **1** to **2**. Moreover, the

change in the substrate whose concentration is varied was found to have significant effects on the apparent K_i values. For example, for the inhibition of lumazine synthase by compound **29**, the K_i value changed from 271 to 852 μM as the substrate with variable concentration changed from **1** to **2**.

The α,α-difluorophosphonate analogue **36** (K_i 132 μM) is similar to the corresponding phosphate **28** (K_i 168 μM) in potency as an inhibitor of lumazine synthase. The phosphate **28** is an uncompetitive inhibitor of lumazine synthase, while the α,α-difluorophosphonate **36** is a partial inhibitor of lumazine synthase. In addition, it should be noted that the α,α-difluorophosphonate **36** was a significantly more potent competitive inhibitor of riboflavin synthase (K_i 39 μM) than the corresponding phosphate **28** (K_i 332 μM). The α,α-difluorophosphonate modification to increase metabolic stability therefore appears to offer the additional advantage of conferring greater activity in some of the present testing systems.

When the potencies of the phosphates **27**−**30** are compared using variable pyrimidinedione substrate **1** concentration, the most potent compound proved to be **27** (K_i 41 μM), in which the phosphate is separated from the purinetrione ring system by a three-carbon linker. That was followed by **30** (K_i 78 μM), **28** (K_i 168 μM), and **29** (K_i 271 μM). In comparison with the other phosphates, the three-carbon linker of **27** makes it the closest structural analogue of the reaction intermediate **5**, and this may explain why it is the most potent lumazine synthase inhibitor.

With variable dihydroxybutanone phosphate substrate **2** concentration, the potencies of **29** (K_i 852 μM) and **30** (K_i 175 μM) can be compared with that of the parent purinetrione **10** (K_i 46 μM), whose enzyme inhibition studies were performed previously with variable substrate **2** concentration.[10] It is interesting to note that the potency of the parent compound **10** (K_i 46 μM) is greater than that of either of the phosphates **29** or **30**, indicating an unexpected opposite of the expected increase in potency anticipated through the incorporation of the phosphate side chains that could bind to the phosphate-binding site of lumazine synthase. One possible explanation for this effect would be that the enzyme kinetics experiments were carried out, as usual, in phosphate buffer, and the inorganic phosphate could conceivably bind to the phosphate-binding site of the enzyme and thus inhibit the binding of **29** and **30**. To examine this hypothesis in more detail, the K_m values for the binding of the dihydroxybutanone phosphate substrate were determined in 50 mM Tris [tris(*C*-hydroxymethyl)aminomethane] buffer, 50 mM MOPS [3-(*N*-morpholino)-propanesulfonic acid] buffer, and 50 mM phosphate buffer, all at pH 7. The K_m values for the substrate **2** were 5.2 ± 0.5 μM in Tris buffer, 6.7 ± 0.4 μM in MOPS buffer, and 50 ± 10 μM in phosphate buffer. Inorganic phosphate therefore does appear to inhibit the binding of the substrate **2**, and most likely the inhibitors **29** and **30**, to lumazine synthase. This could possibly explain why the purinetrione **10** appears to be a better inhibitor than **29** or **30** in phosphate buffer, since the purinetrione does not bind to the phosphate-binding site of the enzyme.

Like the purinetrione **10**, all of the new compounds **27** (K_i 3.63 μM), **28** (K_i 332 μM), **29** (K_i 2.44 μM), **30** (K_i 17.3 μM), and **36** (K_i 39.4 μM) were competitive inhibitors of recombinant *E. coli* riboflavin synthase. However, they are all less potent inhibitors than the purinetrione **10** (K_i 0.61 μM). On the other hand, the previously reported phosphonates **37**, **9**, and **38** were all inactive as riboflavin synthase inhibitors, so the present phosphate and α,α-difluorophosphonate replacements for the phosphonates of these compounds, when combined with attachment to a purinetrione system, do make a positive contribution to the enzyme inhibitory activity.

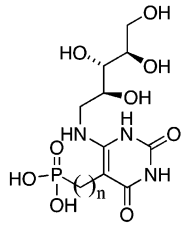

37 n = 4
9 n = 5
38 n = 6

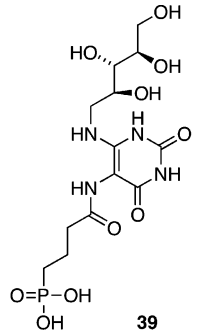

39

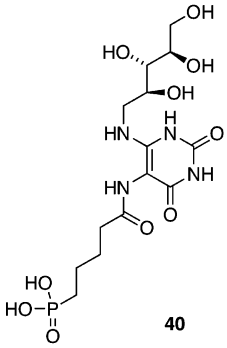

40

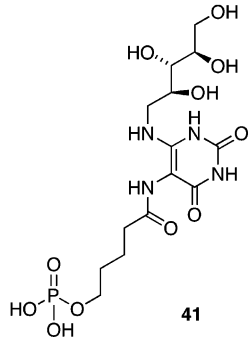

41

Finally, a comparison can be made between the present compounds and the previously reported pyrimidinedione inhibitors **39**, **40**, and **41** having an amide chain connected to phosphonate or phosphate moieties. In contrast to the present series, these amides were inactive or displayed very weak activity vs lumazine synthase, but were riboflavin synthase inhibitors in the K_i 160−190 μM range.[25] All of these compounds are less potent than **27**, **29**, **30**, and **36** vs both lumazine synthase and riboflavin synthase, indicating that the extension of the phosphate or phosphonate side chains from a purinetrione ring system is generally more favorable than connecting them to a pyrimidinedione system through an amide linkage. The one exception is the low activity (K_i 332 μM) displayed by **28** vs riboflavin synthase.

Crystal structures are available of the complexes formed between the substrate analogue **42** and the lumazine synthases of *B. subtilis* and *Schizosaccharomyces pombe*.[26,27] X-ray structures have also been determined of complexes of the intermediate analogue **9** bound

(25) Cushman, M.; Yang, D.; Mihalic, J. T.; Chen, J.; Gerhardt, S.; Huber, R.; Fischer, M.; Kis, K.; Bacher, A. *J. Org. Chem.* **2002**, *67*, 6871−6877.

(26) Ritsert, K.; Huber, R.; Turk, D.; Ladenstein, R.; Schmidt-Bäse, K.; Bacher, A. *J. Mol. Biol.* **1995**, *253*, 151−167.

(27) Gerhardt, S.; Haase, I.; Steinbacher, S.; Kaiser, J. T.; Cushman, M.; Bacher, A.; Huber, R.; Fischer, M. *J. Mol. Biol.* **2002**, *318*, 1317−1329.

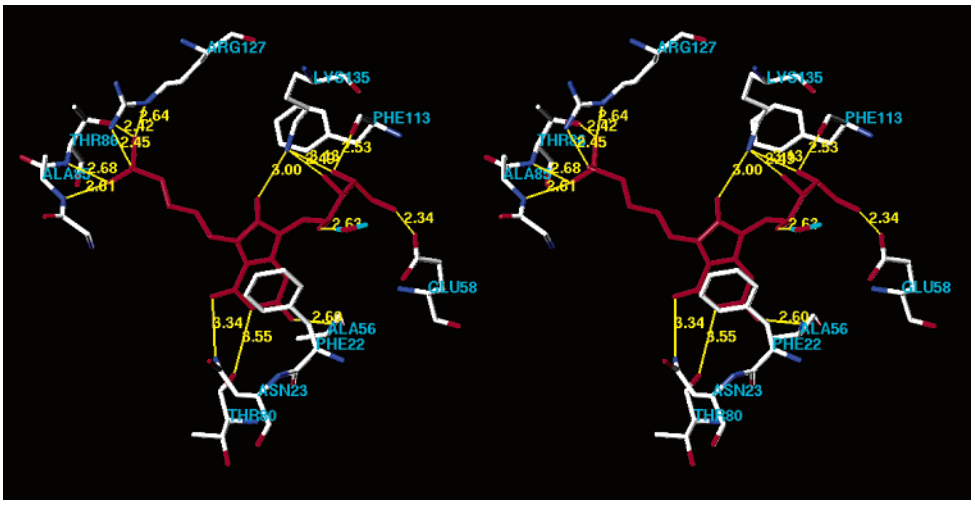

FIGURE 2. Hypothetical model for the binding of compound **27** to *Bacillus subtilis* lumazine synthase. The figure is programmed for walleyed viewing.

to *Saccharomyces cerevisiae* lumazine synthase (Figure 1) and the product analogue **43** bound to *S. pombe* lumazine synthase.[8,27] These structures allow the rational docking and energy minimization of additional lumazine synthase inhibitors. In the present case, a hypothetical model was constructed of the binding of the lumazine synthase/riboflavin synthase inhibitor **27** to *B. subtilis* lumazine synthase. This model was produced by overlapping the structure of **27** with that of **42** in a 15 Å radius spherical fragment surrounding the ligand in one of the sixty equivalent active sites of *B. subtilis* lumazine synthase.[26] The structure of **42** was then removed and the energy of the complex minimized using the MMFF94 force field while allowing the ligand and the protein structure contained within a 6 Å sphere surrounding the ligand to remain flexible with the remainder of the protein structure frozen. The resulting Figure 2 was constructed by displaying the amino acid residues calculated to be involved in bonding of the protein with ligand **27**, using a maximum distance of 3.5 Å between the donor and acceptor atoms to be considered a hydrogen bond. As expected, the calculated structure shows the purinetrione ring of the ligand **27** stacked with the phenyl ring of Phe22. The phosphate of the ligand is extensively hydrogen bonded with the side chain nitrogens of Arg127, as well as the backbone nitrogens of Ala85 and Thr86 and the side-chain hydroxyl of Thr86. The ribityl hydroxyl groups are hydrogen bonded to a water molecule, the side chain amino group of Lys135, the backbone carbonyl of Phe113, and the side chain carboxylate of Glu58. The purinetrione ring of the ligand is hydrogen bonded to the side-chain amino group of Lys135, the backbone nitrogen of Ala56, the backbone carbonyl of Thr80, and the side-chain nitrogen of Asn23. These contacts are summarized in Figure 3. It should be noted that these contacts are either similar or identical to those seen in the crystal structure of **42** bound to *B. subtilis* lumazine synthase.[26]

An X-ray structure of *E. coli* riboflavin synthase, which contains three identical subunits, has been published along with a hypothetical model of the bound substrate 6,7-dimethyl-8-D-ribityllumazine (**3**). In addition, a crystal structure has been determined of a complex formed

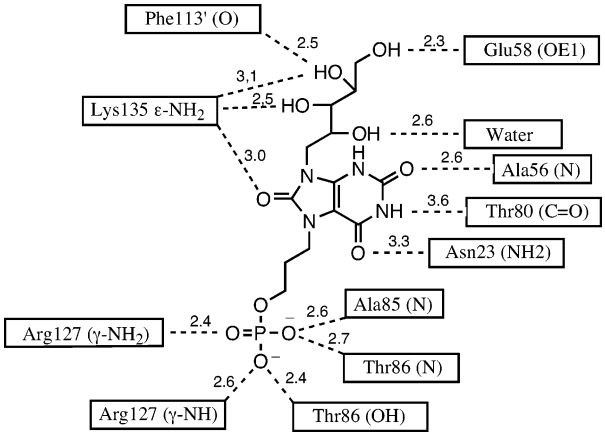

FIGURE 3. Hydrogen bonds and distances in the calculated model of the inhibitor **27** bound in the active site of *Bacillus subtilis* lumazine synthase.

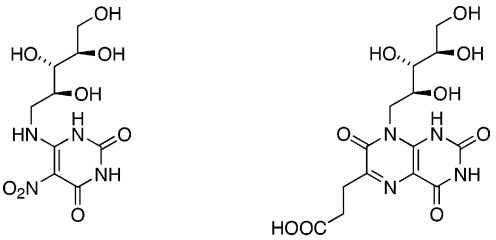

42 **43**

between monomeric *S. pombe* lumazine synthase and 6-carboxyethyl-7-oxo-8-D-ribityllumazine (**43**).[28] According to these studies, as well as NMR investigations of the structure of the N-terminal domain of riboflavin synthase,[29] the active site of the enzyme is derived from the intermolecular juxtaposition of residues belonging to both of the barrels in the C-terminal and N-terminal domains of the two monomer units, with one substrate

(28) Gerhardt, S.; Schott, A.-K.; Kairies, N.; Cushman, M.; Illarionov, B.; Eisenreich, W.; Bacher, A.; Huber, R.; Steinbacher, S.; Fischer, M. *Structure* **2002**, *10*, 1371−1381.

(29) Truffault, V.; Coles, M.; Diericks, T.; Abelmann, K.; Eberhardt, S.; Lüttgen, H.; Bacher, A.; Kessler, H. *J. Mol. Biol.* **2001**, *309*, 949−960.

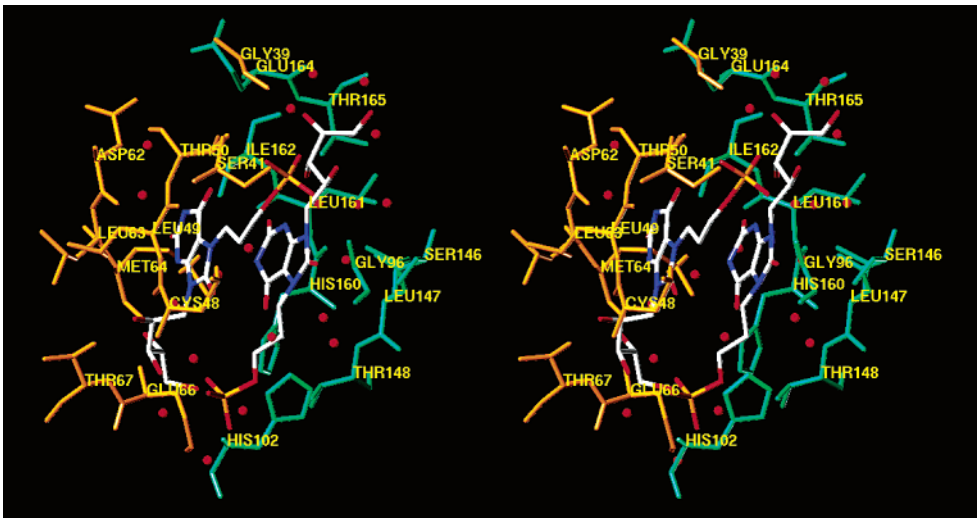

FIGURE 4. Hypothetical model of the binding of two molecules of inhibitor **27** to *Escherichia coli* riboflavin synthase. The C-barrel is orange and the N-barrel is green. Hydrogen atoms have been omitted for clarity. The model is programmed for walleyed viewing.

molecule bound to each barrel. These structures allow molecular modeling of the complex formed between **27** and *E. coli* riboflavin synthase to proceed in a rational way. The structure displayed in Figure 4 was arrived at after docking two molecules of the ligand **27** in the active site and energy minimization using a frozen protein structure and two mobile ligand molecules. The N-barrel residues in Figure 4 are colored orange, while the C-barrel residues are green. As predicted from the known regiochemistry of the riboflavin synthase-catalyzed reaction and the available crystal structures, two molecules of the ligand are stacked in the active site with their ribityl chains pointing in opposite directions.[3] The two phosphate side chains are therefore also pointing in opposite directions, and the model suggests the possibility of hydrogen bonding of each phosphate with some of the ribityl hydroxyl groups of the neighboring ligand molecule.

Human infections with drug-resistant *Mycobacterium tuberculosis* have been an ever-increasing worldwide health problem. New antibiotics that are effective against these resistant strains are therefore needed urgently. Consequently, the phosphates prepared in the present study were also tested vs *M. tuberculosis* lumazine synthase. Also, for the sake of comparison, the parent purinetrione **10** was examined, along with the three-carbon alcohol **46** corresponding to the most potent phosphate **27**. The synthesis of **46** is described in Scheme 6. Alkylation of the starting material **15** with 1,3-diiodopropane in DMF in the presence of potassium carbonate as the base afforded the iodide **44**, which was hydrolyzed to the alcohol **45** with sodium hydroxide in refluxing methanol. Removal of the *tert*-butyldimethylsilyl protecting groups and cleavage of the two methyl ethers present in **45** with methanolic hydrochloric acid yielded the desired product **46**.

As a first step to the determination of the activities of the phosphates **27**−**30** vs *M. tuberculosis* lumazine synthase, an attempt was made to determine the K_m of the phosphate substrate **2**. This proved to be impossible in 100 mM phosphate buffer, because even at a substrate concentration of 1000 μM, the initial reaction velocity still

SCHEME 6[a]

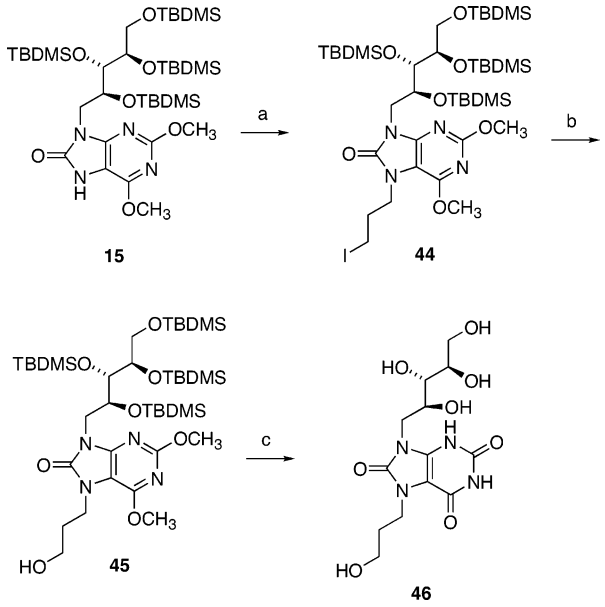

[a] Reagents and conditions: (a) 1,3-diiodopropane, K_2CO_3, DMF, 23 °C (24 h); (b) NaOH, MeOH, reflux (12 h); (c) HCl, MeOH, reflux (3 h).

increased linearly with concentration, indicating that the apparent K_m for the substrate in 100 mM phosphate buffer is much greater than 1000 μM. In contrast, in MOPS buffer (50 mM MOPS pH 7.0, 100 mM NaCl, 5 mM EDTA, 5 mM DTT), maximal reaction velocity was reached by 400 μM phosphate substrate **2** concentration, and in Tris buffer (50 mM Tris−HCl pH 7.0, 100 mM NaCl, 5 mM EDTA, 5 mM DTT), maximal reaction velocity was reached by 250 μM phosphate substrate **2** concentration. Evidently, the *M. tuberculosis* lumazine synthase reaction rate is much more sensitive to inorganic phosphate than the *B. subtilis* enzyme is. For this reason, the subsequent studies on enzyme inhibition by the phosphates **27**−**30** were performed in Tris buffer, using a variable pyrimidinedione **1** concentration and a constant phosphate substrate **2** concentration. As shown

TABLE 2. Inhibition Constants vs *Mycobacterium tuberculosis* Lumazine Synthase[a]

compd	K_i	mechanism
10	9.1 ± 0.61 μM	competitive
46	2.6 ± 0.31 μM	mixed
27	4.5 ± 3.3 nM	competitive
28	4.1 ± 2.3 nM	competitive
29	4.7 ± 1.9 nM	competitive
30	170 ± 1.8 nM	competitive
36	60 ± 6.8 nM	competitive

[a] The experiments were conducted at a fixed substrate **2** concentration of 150 μM and a variable substrate **1** concentration of 1−400 μM.

in Table 2, the resulting K_i values of the phosphates **27**−**29** were all between 4 and 5 *nM*! The phosphate **30**, having the longest phosphate side chain, was less active, displaying a K_i of 0.17 μM. In contrast, the parent purinetrione **10** displayed a K_i of 9.1 μM, the three-carbon alcohol had a K_i of 2.6 μM. It is obvious that the phosphate moieties of the inhibitors **27**−**30** play an important role in increasing the affinity of these enzyme inhibitors for the *M. tuberculosis* lumazine synthase. It is also gratifying to see inhibition constants for the phosphates **27**−**29** in the low nanomolar range vs *M. tuberculosis* lumazine synthase. The crystal structure of *M. tuberculosis* lumazine synthase has not yet been determined, so the structural basis for the differences seen with this enzyme vs the *B. subtilis* enzyme remain to be elucidated.

As mentioned above, a potential limitation of the phosphates **27**−**30** as therapeutically useful antibiotics results from their expected metabolic instability toward phosphatases. Accordingly, the α,α-difluorophosphonate **36** was also tested as an inhibitor of *M. tuberculosis* lumazine synthase. As shown in Table 2, compound **36** displayed a K_i of 60 nM, which is clearly in the range of interest for possible therapeutic use.

In conclusion, the results presented here demonstrate that certain purinetriones bearing phosphate side chains can inhibit both lumazine synthase as well as riboflavin synthase, and molecular modeling with compound **27** suggests possible binding modes to each enzyme. Antibiotics that would inhibit both lumazine synthase and riboflavin synthase would be less likely to suffer from the development of antibiotic resistance by the organisms that they are supposed to treat, since pathogenic microorganisms would have to simultaneously select for mutations in both enzymes in order to escape the cytotoxic effects of the antibiotics.

Experimental Section

General Methods. Melting points were determined in capillary tubes and are uncorrected. Proton nuclear magnetic resonance spectra (^{1}H NMR) were determined at 300 or 500 MHz as noted. Phosphorus nuclear magnetic resonance (^{31}P NMR) chemical shifts are reported relative to 85% H_3PO_4 as external standard. Silica gel used for column chromatography was 230−400 mesh.

6-Chloro-2,4-dimethoxy-5-nitropyrimidine (12). Sulfuric acid (12.5 mL) was added dropwise to fuming nitric acid (7.5 mL) at 0 °C, and 6-chloro-2,4-dimethoxypyrimidine (**11**) (5.00 g, 28.7 mmol) was added. The reaction mixture was stirred at 80−85 °C for 2.5 h, cooled to room temperature, poured into ice−water, and stirred for 20 min. The solid was filtered, washed three times with ice−water, and dried under vacuum to give pure **12** as a yellow solid (4.00 g, 64%): mp 66−67 °C (lit.[15] mp 67−69 °C); ^{1}H NMR (300 MHz, $CDCl_3$) δ 4.07 (s, 3 H), 4.11 (s, 3 H).

2,4-Dimethoxy-5-nitro-6-D-ribitylaminopyrimidine (13). 6-Chloro-2,4-dimethoxy-5-nitropyrimidine (**12**) (5.84 g, 26.85 mmol) was added to a solution of D-ribitylamine (8.83 g, 58.55 mmol) in dry DMF (200 mL), and the mixture was stirred at room temperature for 48 h under nitrogen atmosphere. The solvent was removed using reduced pressure, and the resultant residue was purified using flash chromatography (30 g, 2 × 30 cm column of SiO_2), eluting with chloroform−methanol (10:1), to afford the desired product **13** (7.46 g, 75%) as a light yellow solid: mp 70−71 °C; IR (KBr) 3346, 1598 cm^{-1}; ^{1}H NMR (300 MHz, CD_3OD) δ 4.02 (s, 3 H), 3.99 (s, 3 H), 4.01−3.92 (m, 2 H), 3.80−3.57 (m, 5 H); ^{13}C NMR (75 MHz, CD_3OD) δ 168.4, 164.9, 160.3, 113.3, 79.4, 74.5, 74.2, 71.7, 64.5, 55.9, 55.8, 45.2; EIMS (MH^+) *m*/*z* 335. Anal. Calcd for $C_{11}H_{18}N_4O_8$: C, 39.52; H, 5.43; N, 16.76. Found: C, 39.75; H, 5.32; N, 17.02.

6-(2′,3′,4′,5′-Tetra-*O*-*tert*-butyldimethylsilyl-D-ribitylamino)-2,4-dimethoxy-5-nitropyrimidine (14). Compound **13** (11.5 g, 3.44 mmol), *tert*-butyldimethylsilyl chloride (36.0 g, 24.1 mmol), and imidazole (16.3 g, 24.1 mmol) were dissolved in dry DMF (250 mL), and the mixture was stirred at room temperature for 2 days. DMF was then removed under reduced pressure, and the residue was stirred in ethyl acetate (200 mL) for 2 h. The precipitated salt was filtered, and the filtrate was concentrated to form a yellow oil, which was separated by using flash chromatography (SiO_2), eluting with hexanes−EtOAc (95:5), to afford pure **14** (20.3 g, 75%) as a viscous oil: IR ($CDCl_3$, film) 3356, 2954, 2930, 1594, 1538, 1472, 1361, 1257, 1093 cm^{-1}; ^{1}H NMR (300 MHz, $CDCl_3$) δ 9.00 (s, 1 H), 4.12 (m, 1 H), 4.09 (s, 3 H), 3.95 (s, 3 H), 3.88−3.93 (m, 2 H), 3.82 (dd, J = 2.66 Hz, J = 5.9 Hz, 1 H), 3.69 (dd, J = 5.2 Hz, J = 10.7 Hz, 1 H), 3.50−3.57 (m, 2 H), 0.87 (s, 9 H), 0.86 (s, 9 H), 0.84 (s, 9 H), 0.83 (s, 9 H), 0.10 (s, 3 H), 0.08 (s, 3 H), 0.07 (s. 6 H), 0.03 (s, 6 H), −0.02 (s, 3 H), −0.04 (s, 3 H); EIMS *m*/*z* 791. Anal. Calcd for $C_{35}H_{74}Si_4N_4O_8$: C, 53.12; H, 9.43; N, 7.08. Found: C, 53.22; H, 9.58; N, 6.99.

9-(2′,3′,4′,5′-Tetra-*O*-*tert*-butyldimethylsilyl-D-ribityl)-7,9-dihydro-2,6-dimethoxypurin-8-one (15). Compound **14** (3.80 g, 4.80 mmol) was dissolved in methanol (100 mL), and palladium on charcoal (10%, 0.5 g) was added. The reaction mixture was hydrogenated at room temperature and 1.4 psi for 3 days. The catalyst was filtered off, and the filtrate was concentrated under reduced pressure to remove the methanol completely. The residue was dissolved in dichloromethane (40 mL), and triethylamine (4.00 mL, 28.8 mmol) was added. The mixture was cooled to 0 °C, and a solution of ethyl chloroformate (0.51 mL, 5.28 mmol) in CH_2Cl_2 (10 mL) was added dropwise. The reaction mixture was stirred at room temperature for 6 h, washed with water (2 × 50 mL), dried with anhydrous Na_2SO_4, and concentrated under reduced pressure, and the residue was dried well under vacuum. The residue and NaOEt (820 mg, 12.0 mmol) in absolute EtOH (100 mL) were heated under reflux for 24 h. The solvent was removed under reduced pressure, and compound **15** (1.76 g, 47.0%) was isolated as a solid by flash chromatography (SiO_2, eluting with hexanes−EtOAc 4:1): mp 57−59 °C; IR ($CDCl_3$, film) 3149, 2953, 2928, 2851, 1709, 1635, 1614, 1462, 1375, 1253 cm^{-1}; ^{1}H NMR (500 MHz, $CDCl_3$) δ 9.10 (s, 1 H), 4.48 (d, J = 9.76 Hz, 1 H), 4.30 (dd, J = 10.1, 13.94 Hz, 1 H), 4.06 (dd, J = 1.62, 13.97 Hz, 1 H), 4.01 (s, 4 H), 3.94 (s, 3 H), 3.78 (t, J = 7.14 Hz, 1 H), 3.71 (d, J = 7.15, 10.36 Hz, 1 H), 3.58 (dd, J = 5.60, 10.45 Hz, 1 H), 0.95 (s, 9 H), 0.88 (s, 9 H), 0.87 (s, 9 H), 0.65 (s, 9 H), 0.23 (s, 3 H), 0.13 (s, 3 H), 0.11 (s, 3 H), 0.10 (s, 3 H), 0.049 (s, 3 H), 0.045 (s, 3 H), −0.049 (s, 3 H), −0.47 (s, 3 H); EIMS (MH^+) *m*/*z* 787. Anal. Calcd for $C_{36}H_{74}N_4O_7Si_4$: C, 54.96; H, 9.41; N, 7.12. Found: C, 55.10; H, 9.36; N, 7.06.

General Procedure for the Synthesis of the Iodides 16−18. Compound **15** (394 mg, 0.50 mmol) was dissolved in dry DMF (15 mL). Anhydrous K_2CO_3 (138 mg, 1.00 mmol) and

diiodoalkane (2.25 mmol) were added, and the mixture was stirred under argon at room temperature for 24 h. The DMF was removed under reduced pressure and the residue purified by flash chromatography (SiO_2), eluting with hexanes−EtOAc (95:5), to afford the pure iodides **16**−**18** in 66−94% yields as colorless oils.

4-[9-(2′,3′,4′,5′-Tetra-*O*-*tert*-butyldimethylsilyl-D-ribityl)-7,9-dihydro-2,6-dimethoxy-8-oxopurin-7-yl]-1-iodobutane (16). This intermediate was obtained by the procedure above in 80% yield as a colorless oil: ^{1}H NMR (500 MHz, $CDCl_3$) δ 4.48 (d, J = 9.67 Hz, 1 H), 4.30 (dd, J = 10.08, 13.90 Hz, 1 H), 4.06 (d, J = 1.78 Hz, 2 H), 4.03 (s, 3 H), 3.93 (s, 3 H), 3.90 (m, 2 H), 3.77 (m, 1 H), 3.67 (dd, J = 7.60, 10.35 Hz, 1 H), 3.57 (dd, J = 5.60, 10.45 Hz, 1 H), 3.19 (t, J = 6.41 Hz, 2 H), 1.55 (m, 4 H), 0.94 (s, 9 H), 0.87 (s, 18 H), 0.65 (s, 9 H), 0.20 (s, 3 H), 0.11 (s, 6 H), 0.087 (s, 3 H), 0.042 (s, 3 H), 0.036 (s, 3 H), −0.058 (s, 3 H), −0.48 (s, 3 H); EIMS (MH^+) m/z 969. Anal. Calcd for $C_{40}H_{81}IN_4O_7Si_4$: C, 49.56; H, 8.42; N, 5.78. Found: C, 49.33; H, 7.93; N, 5.24.

5-[9-(2′,3′,4′,5′-Tetra-*O*-*tert*-butyldimethylsilyl-D-ribityl)-7,9-dihydro-2,6-dimethoxy-8-oxopurin-7-yl]-1-iodopentane (17). This compound was obtained by the procedure above in 86% yield as a colorless oil: ^{1}H NMR (300 MHz, $CDCl_3$) δ 4.48 (d, J = 9.75 Hz, 1 H), 4.30 (dd, J = 10.14, 13.92 Hz, 1 H), 4.16 (t, J = 6.53 Hz, 2 H), 4.029 (s, 3 H), 3.93 (s, 3 H), 3.88 (m, 2 H), 3.76 (m, 1 H), 3.67 (dd, J = 7.60, 10.35 Hz, 1 H), 3.56 (dd, J = 5.60, 10.45 Hz, 1 H), 3.16 (t, J = 6.53 Hz, 2 H), 1.84 (m, 2 H), 1.69 (m, 2 H), 1.50−1.40 (m, 2 H), 0.94 (s, 9 H), 0.87 (s, 18 H), 0.64 (s, 9 H), 0.20 (s, 3 H), 0.107 (s, 6 H), 0.087 (s, 3 H), 0.042 (s, 3 H), 0.036 (s, 3 H), −0.060 (s, 3 H), −0.49 (s, 3 H); EIMS (MH^+) m/z 983. Anal. Calcd for $C_{41}H_{83}IN_4O_7Si_4 \cdot C_6H_{14}$: C, 52.74; H, 9.07; N, 5.23. Found: C, 52.92; H, 8.71; N, 4.96.

6-[9-(2′,3′,4′,5′-Tetra-*O*-*tert*-butyldimethylsilyl-D-ribityl)-7,9-dihydro-2,6-dimethoxy-8-oxopurin-7-yl]-1-iodohexane (18). This compound was obtained by the procedure above in 94% yield as a colorless oil: IR (neat) 2935, 2864, 1717, 1628 cm^{-1}; ^{1}H NMR (300 MHz, $CDCl_3$) δ 4.47 (d, J = 9.54 Hz, 1 H), 4.39 (dd, J = 9.98, 13.81 Hz, 1 H), 4.06 (d, J = 1.96 Hz, 2 H), 4.02 (s, 3 H), 3.92 (s, 3 H), 3.86 (m, 2 H), 3.77 (m, 1 H), 3.67 (dd, J = 7.58, 10.31 Hz, 1 H), 3.56 (dd, J = 5.62, 10.40 Hz, 1 H), 3.15 (t, J = 6.96 Hz, 2 H), 1.79 (qn, 2 H), 1.67 (qn, 2 H), 1.38 (m, 4 H), 0.93 (s, 9 H), 0.87 (s, 18 H), 0.64 (s, 9 H), 0.20 (s, 3 H), 0.10 (s, 6 H), 0.080 (s, 3 H), 0.035 (s, 3 H), 0.029 (s, 3 H), −0.066 (s, 3 H), −0.49 (s, 3 H); EIMS (MH^+) m/z 997. Anal. Calcd for $C_{42}H_{85}IN_4O_7Si_4$: C, 50.60; H, 8.53; N, 5.62. Found: C, 50.22; H, 8.71; N, 5.45.

Dibenzyl 3-[9-(2′,3′,4′,5′-Tetra-*O*-*tert*-butyldimethylsilyl-D-ribityl)-7,9-dihydro-2,6-dimethoxy-8-oxopurin-7-yl]-propane 1-Phosphate (19). Compound **15** (0.551 g, 0.70 mmol) was dissolved in dry DMF (20 mL) under an atmosphere of argon. Anhydrous K_2CO_3 (0.495 g, 3.58 mmol) and compound **32** (0.313 g, 0.70 mmol) were added, and the mixture was stirred at room temperature for 24 h. Excess solvent was removed using reduced pressure, and the residue was purified by using flash chromatography (28 g, 5 × 40 cm column of SiO_2), eluting with hexanes−ethyl acetate (80:20), to furnish **19** (0. 512 g, 66%) as colorless oil: IR (neat) 2954, 1716, 1627 cm^{-1}; ^{1}H NMR (300 MHz, $CDCl_3$) δ 7.33−7.29 (m, 10 H), 5.01 (m, 4 H), 4.46 (d, J = 9.58 Hz, 1 H), 4.29 (dd, J = 10.04, 13.95 Hz, 1 H), 4.09−3.96 (m, 5 H), 3.94 (s, 4 H), 3.92 (s, 3 H), 3.76 (m, 1 H), 3.66 (dd, J = 7.60, 10.35 Hz, 1 H), 3.55 (dd, J = 5.60, 10.45 Hz, 1 H), 2.01 (m, 2 H), 0.94 (s, 9 H), 0.87 (s, 18 H), 0.63 (s, 9 H), 0.20 (s, 3 H), 0.10 (s, 6 H), 0.08 (s, 3 H), 0.039 (s, 3 H), 0.033 (s, 3 H), −0.068 (s, 3 H), −0.52 (s, 3 H); EIMS (MH^+) m/z 1105. Anal. Calcd for $C_{53}H_{93}PN_4O_{11}Si_4$: C, 57.61; H, 8.42; N, 5.07. Found: C, 57.29; H, 8.23; N, 4.83.

General Procedure for the Synthesis of Dibenzyl Phosphates 20−22. Compounds **16**, **17**, or **18** (0.95 mmol) and silver dibenzyl phosphate (0.366 g, 0.95 mmol) were heated at reflux in dry acetonitrile (20 mL) for 8 h under an atmosphere of argon. The solutions were filtered and concentrated under reduced pressure. The resultant oils were purified by flash chromatography (28 g, 5 × 40 cm column of SiO_2), eluting with hexanes−ethyl acetate (7:3), to furnish the products as colorless oils.

Dibenzyl 4-[9-(2′,3′,4′,5′-Tetra-*O*-*tert*-butyldimethylsilyl-D-ribityl)-7,9-dihydro-2,6-dimethoxy-8-oxopurin-5-yl]-butane 1-Phosphate (20). Compound **20** was obtained by the procedure above in 83% yield as a colorless oil: ^{1}H NMR (300 MHz, $CDCl_3$) δ 7.31 (s, 10 H), 5.01 (m, 4 H), 4.47 (d, J = 9.9 Hz, 1 H), 4.30 (dd, J = 10.08, 13.90 Hz, 1 H), 4.06 (d, J = 1.78 Hz, 1 H), 4.02 (d, J = 2.1 Hz, 2 H), 3.99 (s, 1 H), 3.96 (s, 3 H), 3.96 (s, 3 H), 3.84 (m, 2 H), 3.77 (m, 1 H), 3.66 (dd, J = 5.60, 10.45 Hz, 1 H), 3.56 (dd, J = 5.8, 10.35 Hz, 1 H), 1.72 (m, 4 H), 0.94 (s, 9 H), 0.87 (s, 18 H), 0.63 (s, 9 H), 0.20 (s, 3 H), 0.11 (s, 6 H), 0.09 (s, 3 H), 0.043 (s, 3 H), 0.041 (s, 3 H), −0.071 (s, 3 H), −0.52 (s, 3 H); EIMS (MH^+) m/z 1119. Anal. Calcd for $C_{54}H_{94}N_4O_{11}PSi_4$: C, 57.93; H, 8.55; N, 5.00. Found: C, 58.00; H, 8.65; N, 5.08.

Dibenzyl 5-[9-(2′,3′,4′,5′-Tetra-*O*-*tert*-butyldimethylsilyl-D-ribityl)-7,9-dihydro-2,6-dimethoxy-8-oxopurin-7-yl]-pentane 1-Phosphate (21). Intermediate **21** was obtained by the procedure above in 64% yield as a colorless oil: ^{1}H NMR (300 MHz, $CDCl_3$) δ 7.32 (m, 10 H), 5.01 (m, 4 H), 4.48 (d, J = 9.63 Hz, 1 H), 4.47 (dd, J = 10.14, 13.92 Hz, 1 H), 4.07 (d, J = 2.06 Hz, 1 H), 4.029 (br s, 1 H), 3.98 (s, 3 H), 3.96 (m, 1 H), 3.94 (m, 1 H), 3.93 (s, 3 H), 3.81 (m, 3 H), 3.67 (dd, J = 5.60, 10.45 Hz, 1 H), 3.56 (dd, J = 5.8, 10.35 Hz, 1 H), 1.62 (m, 4 H), 1.33 (m, 2 H), 0.94 (s, 9 H), 0.87 (s, 18 H), 0.64 (s, 9 H), 0.20 (s, 3 H), 0.107 (s, 6 H), 0.085 (s, 3 H), 0.042 (s, 3 H), 0.036 (s, 3 H), −0.064 (s, 3 H), −0.507 (s, 3 H); EIMS (M^+) m/z 1132. Anal. Calcd for $C_{55}H_{97}PN_4O_{11}Si_4$: C, 58.30; H, 8.57; N, 4.95. Found: C, 58.28; H, 8.40; N, 4.89.

Dibenzyl 6-[9-(2′,3′,4′,5′-Tetra-*O*-*tert*-butyldimethylsilyl-D-ribityl)-7,9-dihydro-2,6-dimethoxy-8-oxopurin-5-yl]-hexane 1-Phosphate (22). The phosphate **22** was obtained by the procedure above in 58% yield as a colorless oil: IR (neat) 2943, 2864, 1717, 1628 cm^{-1}; ^{1}H NMR (300 MHz, $CDCl_3$) δ 7.31 (s, 10 H), 5.01 (m, 4 H), 4.47 (d, J = 9.31 Hz, 1 H), 4.30 (dd, J = 9.99, 13.86 Hz, 1 H), 4.08 (d, J = 1.78 Hz, 1 H), 4.02 (m, 1 H), 3.99 (s, 3 H), 3.96 (s, 1 H), 3.96 (s, 3 H), 3.93 (t, J = 2.40 Hz, 1 H), 3.82 (m, 3 H), 3.68 (dd, J = 7.54, 10.34 Hz, 1 H), 3.56 (dd, J = 5.8, 10.35 Hz, 1 H), 1.61 (m, 4 H), 1.30 (m, 4 H), 0.94 (s, 9 H), 0.87 (s, 18 H), 0.64 (s, 9 H), 0.20 (s, 3 H), 0.11 (s, 6 H), 0.095 (s, 3 H), 0.041 (s, 3 H), 0.034 (s, 3 H), −0.064 (s, 3 H), −0.50 (s, 3 H); ^{13}C NMR (75 MHz, $CDCl_3$) δ 159.8, 153.5, 153.0, 151.4, 135.9, 135.8, 128.5, 128.4, 127.8, 102.0, 77.6, 69.1, 69.0, 67.8, 67.7, 64.6, 60.3, 54.8, 53.8, 43.67, 42.3, 30.0, 29.6, 26.0, 25.9, 25.6, 18.3, 18.1, 17.5, −4.2, −4.3, −4.4, −4.6, −5.3, −5.4, −5.8; ^{31}P NMR (121 MHz, $CDCl_3$) δ −0.28; EIMS (MH^+) m/z 1147. Anal. Calcd for $C_{56}H_{99}PN_4O_{11}Si_4$: C, 58.63; H, 8.63; N, 4.88. Found: C, 58.52; H, 8.56; N, 4.86.

General Procedure for the Synthesis of Intermediates 23−26. Compounds **19**−**22** (0.46 mmol) were dissolved in dry THF (12 mL) and transferred to dry polyethylene vials equipped with rubber septa and a magnetic stirring bars. The cold (0 °C), magnetically stirred solutions were treated under argon with HF−Py (2 mL) and stirred 1 h, and then the ice bath was removed. Stirring was continued for another 6 h, HF−Py (2 mL) was added again, and the mixtures were stirred for 12 h. The cold (0 °C) solutions were diluted with ether (50 mL) and neutralized with saturated $NaHCO_3$ solution (10 mL), and then solid $NaHCO_3$ was added slowly until the mixture reached pH 7. The solutions were filtered, the filtrates were extracted with chloroform (3 × 15 mL), and the extracts were combined and concentrated. The residues were purified by silica gel column chromatography (15 g, 3 × 30 cm column of SiO_2), eluting with $CHCl_3$−MeOH (9:1), to afford the desired compounds **23**−**26** as colorless oils.

Dibenzyl 3-(7,9-Dihydro-2,6-dimethoxy-8-oxo-9-D-ribitylpurin-7-yl)propane 1-Phosphate (23). This product was obtained by the above procedure in 58% yield: IR (neat) 3384, 2953, 1696 cm^{-1}; ^{1}H NMR (500 MHz, $CDCl_3$) δ 7.31−7.28 (m,

10 H), 5.02−4.94 (m, 4 H), 4.18 (br s, 2 H), 4.09−4.05 (m, 2 H), 4.02−3.93 (m, 4 H), 3.95 (s, 3 H), 3.89 (s, 3 H), 3.79 (m, 2 H), 3.73 (m, 1 H), 3.48 (q, J = 6.31 Hz, 1 H), 1.99 (m, 2 H); ^{31}P NMR (121 MHz, $CDCl_3$) δ −0.25; EIMS (MH^+) m/z 649. Anal. Calcd for $C_{29}H_{37}N_4O_{11}P\cdot0.7H_2O$: C, 52.63; H, 5.81; N, 8.47. Found: C, 52.58; H, 5.91; N, 8.28.

Dibenzyl 4-(7,9-Dihydro-2,6-dimethoxy-8-oxo-9-D-ribitylpurin-7-yl)butane 1-Phosphate (24). This intermediate was obtained by the above procedure in 43% yield: ^{1}H NMR (300 MHz, $CDCl_3$) δ 7.27 (s, 10 H), 4.94 (dd, J = 12.5 and 20.7 Hz, 4 H), 4.78 (br s, 1 H), 4.17 (m, 2 H), 4.07 (m, 2 H), 3.96 (s, 3 H), 3.94 (m, 3 H), 3.87 (s, 3 H), 3.85 (m, 3 H), 3.75 (br s, 2 H), 3.47 (t, J = 6.7 Hz, 1 H), 1.68 (m, 2 H), 1.59 (m, 2 H); ^{13}C NMR (75 MHz, $CDCl_3$) δ 159.8, 153.8, 153.7, 151.1, 135.6, 135.5, 128.4, 127.8, 102.0, 73.3, 72.3, 71.7, 69.2, 69.1, 67.2, 67.1, 63.5, 54.9, 54.1, 43.4, 42.0, 26.9, 25.6; EIMS (MNa^+) m/z 685. Anal. Calcd for $C_{30}H_{39}N_4O_{11}P\cdot0.5H_2O$: C, 53.60; H, 5.95; N, 8.34. Found: C, 53.50; H, 5.76; N, 8.30.

Dibenzyl 5-(7,9-Dihydro-2,6-dimethoxy-8-oxo-9-D-ribitylpurin-7-yl)pentane 1-Phosphate (25). This intermediate was obtained by the above procedure in 80% yield: IR (neat) 3382, 2952, 1697 cm^{-1}; ^{1}H NMR (300 MHz, $CDCl_3$) δ 7.26 (s, 10 H), 4.93 (m, 4 H), 4.81 (br s, 1 H), 4.42 (br s, 1 H), 4.23−4.08 (m, 4 H), 3.97 (s, 3 H), 3.95−3.81 (m, 6 H), 3.87 (s, 3 H), 3.75 (s, 2 H), 3.49 (br s, 1 H), 1.60 (m, 4 H), 1.30 (m, 2 H); ^{13}C NMR (75 MHz, $CDCl_3$) δ 159.6, 153.6, 153.5, 151.0, 135.5, 135.4, 128.3, 127.6, 101.9, 73.2, 72.1, 71.7, 69.0, 69.0, 67.5, 67.4, 63.4, 43.2, 42.2, 29.3, 29.2, 28.9, 22.0; EIMS (MH^+) m/z 677. Anal. Calcd for $C_{31}H_{41}N_4O_{11}P\cdot0.2H_2O$: C, 54.68; H, 6.08; N, 8.23. Found: C, 54.67; H, 6.27; N, 7.93.

Dibenzyl 6-(7,9-Dihydro-2,6-dimethoxy-8-oxo-9-D-ribitylpurin-7-yl)hexane 1-Phosphate (26). This product was obtained by the above procedure in 58% yield: ^{1}H NMR (300 MHz, $CDCl_3$) δ 7.30 (s, 10 H), 4.98 (dd, J = 12.97 and 20.89 Hz, 4 H), 4.24 (br s, 2 H), 4.04 (m, 2 H), 4.03 (s, 3 H), 3.96−3.82 (m, 6 H), 3.93 (s, 3 H), 3.77 (d, J = 3.98 Hz, 2 H), 3.38 (t, J = 6.44 Hz, 2 H), 1.66 (qn, J = 6.36 Hz, 2 H), 1.57 (qn, J = 6.69 Hz, 2 H), 1.29 (m, 4 H); ^{13}C NMR (75 MHz, $CDCl_3$) δ 159.7, 153.7, 153.6, 151.0, 135.6, 135.5, 128.3, 127.7, 102.0, 73.1, 71.9, 71.8, 69.1, 69.0, 67.2, 67.1, 63.4, 54.8, 53.9, 43.2, 42.4, 29.8, 29.7, 29.4, 25.1, 24.7; ^{31}P NMR (121 MHz, $CDCl_3$) δ −0.26; EIMS (MNa^+) m/z 713. Anal. Calcd for $C_{32}H_{43}N_4O_{11}P\cdot0.5H_2O$: C, 54.93; H, 6.34; N, 8.00. Found: C, 55.00; H, 6.37; N, 7.96.

3-(1,3,7,9-Tetrahydro-9-D-ribityl-2,6,8-trioxopurin-7-yl)propane 1-Phosphate (27). Compound **23** (310 mg, 0.48 mmol) was dissolved in a mixture of concd HCl (5 mL) and methanol (5 mL), and the mixture was heated at reflux for 3 h. The solvent was removed by vacuum distillation to result in a very small volume. Methanol (3 × 20 mL) was added and distilled off. The residue was dissolved in 2-propanol−methanol (10:1) at reflux, and the solution was then cooled to room temperature and the precipitate was collected by filtration. The solid was dissolved in deionized water, and the clear water solution was lyophilized to result in a white solid, which was dried under vacuum to afford **27** (132 mg, 60%) as a white hygroscopic solid: ^{1}H NMR (300 MHz, D_2O) δ 4.11−3.66 (m, 11H), 2.07 (m, 2 H); ^{13}C NMR (75 MHz, D_2O) δ 155.2, 152.4, 151.5, 139.0, 98.5, 72.2, 69.5, 64.3, 62.6, 44.5, 40.1, 30.0; ESIMS m/z 441 (MH^+); HRMS calcd for $C_{13}H_{21}N_4O_{11}P$ 440.1023, found 440.1017. Anal. Calcd for $C_{13}H_{21}N_4O_{11}P\cdot0.2\ (CH_3)_2CHOH$: C, 36.11; H, 5.04; N, 12.38. Found: C, 35.98; H, 5.10; N, 12.14.

4-(1,3,7,9-Tetrahydro-9-D-ribityl-2,6,8-trioxopurin-7-yl)butane 1-Phosphate (28). Compound **24** (240 mg, 0.21 mmol) was dissolved in a mixture of concd HCl (3 mL) and methanol (3 mL), and the mixture was heated at reflux for 3 h. The solvent was removed by vacuum distillation, and the residue was first separated by flash chromatography (SiO_2), eluting with MeOH−CH_2Cl_2−H_2O−AcOH (7:4:2:1), and then further purified with Dowex 50 1 × 8 anion-exchange resin, eluting with 1.5% aq HCl. The fraction which contained the product was concentrated under reduced pressure to a very small volume, and methanol (3 × 20 mL) was added and distilled off. The residue was dissolved in deionized water. The clear aqueous solution was lyophilized to result in a white solid, which was dried under vacuum to afford **28** as a white hygroscopic solid (60 mg, 63%): ^{1}H NMR (300 MHz, D_2O) δ 4.07−3.54 (m, 11 H), 1.75−1.57 (m, 4 H); ^{13}C NMR (75 MHz, D_2O) δ 155.5, 152.9, 151.9, 139.3, 98.7, 73.0, 72.4, 69.8, 67.2, 62.8, 44.5, 42.2, 26.7, 25.3; ESIMS m/z 455 (MH^+); HRMS calcd for $C_{14}H_{23}N_4O_{11}P$ 454.1179, found 454.1172. Anal. Calcd for $C_{14}H_{23}N_4O_{11}P\cdot0.3H_2O$: C, 36.54; H, 5.13; N, 12.18. Found: C, 36.54; H, 5.12; N, 11.81.

Dibenzyl 3-Iodopropyl 1-Phosphate (32). A mixture of 1,3-diiodopropane (1.20 mL, 10.4 mmol) and silver dibenzyl phosphate (1.20 g, 3.13 mmol) in dry acetonitrile (30 mL) was heated at reflux under argon for 10 h. The reaction mixture was filtered, the filtrate was concentrated under reduced pressure, and the residue was separated with flash chromatography (SiO_2, 230−400 mesh) (elution: hexanes−EtOAc 4:1) to afford pure **32** (1.05 g, 86.0%) as colorless oil: ^{1}H NMR (300 MHz, $CDCl_3$) δ 7.34 (s, 10 H), 5.03 (m, 4 H), 4.02 (q, J = 6.14 Hz, 2 H), 3.12 (t, J = 6.75 Hz, 2 H), 2.03 (m, 2 H).

Diethyl 5-[9-(2′,3′,4′,5′-Tetra-*O*-*tert*-butyldimethylsilyl-D-ribityl)-7,9-dihydro-2,6-dimethoxy-8-oxopurin-7-yl]-1,1-difluoropentane 1-Phosphonate (34). Compound **15** (1.00 g, 1.27 mmol) was dissolved in dry DMF (30 mL) under an atmosphere of argon. Anhydrous K_2CO_3 (0.898 g) and compound **33**[24] (0.469 g, 1.27 mmol) were added, and the mixture was stirred at room temperature for 24 h. Excess solvent was removed using reduced pressure, and the residue was purified by using flash chromatography (28 g, 5 × 40 cm column of SiO_2), eluting with hexanes−ethyl acetate (80:20), to furnish **34** (1.24 g, 95%) as colorless oil: ^{1}H NMR (500 MHz, $CDCl_3$) δ 4.48 (d, J = 9.70 Hz, 1 H), 4.29 (dd, J = 10.17, 13.95 Hz, 1 H), 4.23 (q, J = 7.31 Hz, 4 H), 4.09−4.02 (m, 2 H), 4.02 (s, 3 H), 3.93 (s, 3 H), 3.89 (m, 2 H), 3.77 (m, 1 H), 3.68 (dd, J = 7.78, 10.35 Hz, 1 H), 3.56 (dd, J = 5.62, 10.5 Hz, 1 H), 2.07 (m, 2 H), 1.74 (m, 2 H), 1.63 (m, 2 H), 1.35 (t, J = 7.05 Hz, 6 H), 0.94 (s, 9 H), 0.87 (s, 18 H), 0.64 (s, 9 H), 0.20 (s, 3 H), 0.11 (s, 6 H), 0.087 (s, 3 H), 0.043 (s, 3 H), 0.036 (s, 3 H), −0.061 (s, 3 H), −0.49 (s, 3 H); EIMS (MH^+) m/z 1029. Anal. Calcd for $C_{45}H_{91}F_2N_4O_{10}PSi_4$: C, 52.50; H, 8.91; N, 5.44. Found: C, 52.11; H, 8.72, N, 5.33.

Diethyl 5-(5,7-Dihydro-2,4-dimethoxy-8-oxo-9-D-ribitylpurin-5-yl)-1,1-difluoropentane 1-Phosphonate (35). Compound **34** (1.23 g, 1.19 mmol) was dissolved in dry THF (20 mL) and the solution transferred to a dry polyethylene vial equipped with a rubber septum and a magnetic stirring bar. The cold (0 °C), magnetically stirred solution was treated under argon with HF−Py (5.2 mL) and stirred for 1 h, and then the ice bath was removed. Stirring was continued for another 6 h, HF−Py (5.2 mL) was added again, and the mixture was stirred overnight. The cold solution (0 °C) was diluted with ether (50 mL) and neutralized with saturated $NaHCO_3$ solution. The solution was filtered, and the filtrate was lyophilized. The residue was purified by silica gel column chromatography (15 g, 3 × 30 cm column of SiO_2), eluting with $CHCl_3$−MeOH (9:1) to afford desired compound **35** (0.309 g, 46%): ^{1}H NMR (300 MHz, $CDCl_3$) δ 4.79 (br s, 1 H), 4.69 (br s, 1 H), 4.25−4.13 (m, 7 H), 4.00 (s, 4 H), 3.88 (s, 4 H), 3.79 (br s, 1 H), 3.72 (br s, 2 H), 3.42 (br s, 1 H), 2.11−1.92 (m, 2 H), 1.72 (m, 2 H), 1.55 (m, 2 H), 1.29 (t, J = 7.06 Hz, 6 H); ^{13}C NMR (75 MHz, $CDCl_3$) δ 159.8, 153.8, 153.7, 151.1, 73.3, 72.4, 71.6, 64.5, 64.4, 63.5, 54.9, 54.1, 43.4, 42.2, 33.2 (q), 29.1, 17.6, 16.2, 16.2; EIMS (MH^+) m/z 573. Anal. Calcd for $C_{21}H_{35}F_2N_4PO_{10}$: C, 44.06; H, 6.16. Found: C, 44.02; H, 6.18.

5-(1,3,7,9-Tetrahydro-9-D-ribityl-2,6,8-trioxopurin-7-yl)-1,1-difluoropentane 1-Phosphonate (36). To a solution of compound **35** (0.309 g, 0.54 mmol) in dry CH_2Cl_2 (10 mL) was added trimethylsilyl iodide (0.23 mL), and the reaction mixture was stirred at room temperature for 24 h under argon atmosphere. Water (15 mL) was added and the mixture stirred

at room temperature for 10 h and washed with CH_2Cl_2 (3 × 10 mL). The water layer was lyophilized, resulting in **36** as a colorless solid (0.235 g, 89%): mp 92−94 °C; ^{1}H NMR (300 MHz, D_2O) δ 3.85 (m, 2 H), 3.73 (m, 3 H), 3.65 (m, 1 H), 3.57 (d, J = 2.89 Hz, 1 H), 3.53−3.42 (m, 2 H), 1.86 (m, 2 H), 1.56 (quint, J = 6.93 Hz, 2 H), 1.35 (quint, J = 6.29 Hz, 2 H); EIMS (MH^+) m/z 489. Anal. Calcd for $C_{15}H_{23}N_4F_2O_{10}P\cdot1.5H_2O$: C, 32.19; H, 4.26. Found: C, 32.10; H, 4.60.

3-[9-(2′,3′,4′,5′-Tetra-*O*-*tert*-butyldimethylsilyl-D-ribityl)-7,9-dihydro-2,6-dimethoxy-8-oxopurin-7-yl]-1-iodopropane (44). This compound was prepared using the general procedure described above for iodides **16**−**18**: ^{1}H NMR (300 MHz, $CDCl_3$) δ 5.10 (dd, J = 9.91, 3.09 Hz, 1 H), 4.41 (m, 4 H), 4.00 (m, 7 H), 3.80 (m, 1 H), 3.68 (m, 1 H), 3.57 (m, 3 H), 1.96 (m, 2 H), 0.86 (m, 27 H), 0.59 (s, 9 H), 0.10−0.06 (m, 21 H), −0.51 (s, 3 H). Anal. Calcd for $C_{39}H_{71}IN_4O_7Si_4$: C, 49.03; H, 8.34; N, 5.86. Found: C, 48.99; H, 7.92; N, 5.46.

3-[9-(2′,3′,4′,5′-Tetra-*O*-*tert*-butyldimethylsilyl-D-ribityl)-5,7-dihydro-2,4-dimethoxy-8-oxopurin-5-yl]-1-propanol (45). Compound **44** (238 mg, 0.25 mmol) was dissolved in a solution of 1 N NaOH−MeOH (1:1, 10 mL), and the mixture was heated at reflux for 12 h. The solvent was distilled off under reduced pressure and the residue was purified by flash chromatography (SiO_2), eluting with hexanes−ethyl acetate (5:1), to furnish compound **45** (160 mg, 75%) as a colorless oil: ^{1}H NMR (300 MHz, $CDCl_3$) δ 5.00 (dd, J = 9.96, 3.11 Hz, 1 H), 4.29 (m, 4 H), 4.03 (s, 3 H), 3.91 (m, 4 H), 3.74 (m, 1 H), 3.61 (m, 1 H), 3.47 (m, 1 H), 3.13 (t, J = 6.69 Hz, 2 H), 2.13 (m, 2 H), 0.84−0.77 (m, 27 H), 0.52 (s, 9 H), 0.06−0.05 (m, 18 H), 0.14 (s, 3 H), −0.59 (s, 3 H). Anal. Calcd for $C_{39}H_{80}N_4O_8Si_4$: C, 55.41; H, 9.54; N, 6.63. Found: C, 55.12; H, 9.38; N, 6.24.

3-(1,3,7,9-Tetrahydro-9-D-ribityl-2,6,8-trioxopurin-7-yl)-1-propanol (46). Compound **45** (150 mg, 0.18 mmol) was dissolved in a solution of concd HCl−MeOH (1:1, 10 mL), and the mixture was heated at reflux for 3 h. The solvent was removed under reduced pressure, and the residue was reprecipitated from propanol. The solid was dried under vacuum to afford **46** (25 mg, 35%) as a white solid: mp 187−188 °C; ^{1}H NMR (300 MHz, D_2O) δ 3.92 (m, 5 H), 3.66 (m, 6 H), 1.80 (m, 2 H); MS (ESI) 359 (M − 1). Anal. Calcd for $C_{13}H_{20}N_4O_8\cdot2.5H_2O$: C, 38.51; H, 6.17; N, 13.82. Found: C, 38.23; H, 5.72; N, 13.44.

Molecular Modeling on Lumazine Synthase. Using Sybyl (Tripos, Inc., version 6.9, 2002), the X-ray crystal structure of the complex of 5-nitro-6-ribitylamino-2,4-(1*H*,3*H*)-pyrimidinedione (**42**) and the lumazine synthase of *B. subtilis* (1RVV)[26] was clipped to include information within a 15 Å radius of one of the 60 equivalent ligand molecules. The residues that were clipped in this cut complex were capped with either neutral amino or carboxyl groups. The structure of the inhibitor **27** was overlapped with the structure of 5-nitro-6-ribitylamino-2,4-(1*H*,3*H*)-pyrimidinedione (**42**), which was then deleted. Hydrogen atoms were added to the complex. MMFF94 charges were loaded, and the energy of the complex was minimized using the Powell method to a termination gradient of 0.05 kcal/mol while employing the MMFF94 force field. During the minimization of the complex, inhibitor **27** and the 6 Å sphere surrounding it were allowed to remain flexible, while the remaining portion of the complex was held ridged using the aggregate function. Figure 2 was constructed by displaying the amino acid residues of the enzyme that are involved in hydrogen bonding with the inhibitor **27**. The maximum distance between donor and acceptor atoms contributing to the hydrogen bonds shown in Figure 1 was set to 3.5 Å.

Molecular Modeling on Riboflavin Synthase. Using Sybyl (Tripos, Inc., version 6.9, 2002), the X-ray crystal structure of *E. coli* riboflavin synthase (1I8D) was downloaded and two molecules of the ligand **27** were docked and oriented as suggested by the published model of the binding of two molecules of the substrate **1** in the active site,[30] as well as by the structure of **43** bound to *S. pombe* riboflavin synthase.[28] The C- and N-terminal groups were changed to neutral carboxylic acid and amino groups, and hydrogens were added to the protein structure and to the oxygens of the water molecules. MMFF94 charges were loaded, and the energy of a 6 Å radius spherical subset including and surrounding the two ligand molecules was minimized using the Powell method to a termination gradient of 0.05 kcal/mol while employing the MMFF94 force field. During energy minimization, the remaining protein structure was held rigid using the aggregate function. Figure 4 was constructed by displaying the amino acid residues in the C- and N-barrels surrounding the two ligand molecules.

Lumazine Synthase Assay.[31] Reaction mixtures contained 100 mM potassium phosphate, pH 7.0, 5 mM EDTA, 5 mM dithiothreitol, inhibitor (0−500 μM), 170 μM 5-amino-6-ribitylamino-2,4(1*H*,3*H*)-pyrimidinedione (**1**) and *B. subtilis* lumazine synthase (16 μg, specific activity 8.5 μmol mg^{-1} h^{-1}) in a total volume of 1000 μL. The solution was incubated at 37 °C, and the reaction was started by the addition of a small volume (20 μL) of L-3,4-dihydroxy-2-butanone 4-phosphate (**2**) to a final concentration of 50−400 μM. The formation of 6,7-dimethyl-8-ribityllumazine (**3**) was measured online with a computer-controlled photometer at 408 nm ($\epsilon_{lumazine}$ = 10 200 M^{-1} cm^{-1}). The velocity−substrate data were fitted for all inhibitor concentrations with a nonlinear regression method using the program DynaFit.[32] Different inhibition models were considered for the calculation. K_i values ± standard deviations were obtained from the fit under consideration of the most likely inhibition model. In a separate set of experiments, the L-3,4-dihydroxy-2-butanone 4-phosphate concentration (**2**) was kept constant at 100 μM and the concentration of the second substrate, 5-amino-6-ribitylamino-2,4(1*H*,3*H*)-pyrimidinedione (**1**), was varied.

Riboflavin Synthase Assay.[33] Reaction mixtures contained buffer (100 mM potassium phosphate, 10 mM EDTA, 10 mM sodium sulfite), inhibitor (0 to 300 μM), and riboflavin synthase (4.6 μg, specific activity 45 μmol mg^{-1} h^{-1}). After preincubation, the reactions were started by the addition of various amounts of 6,7-dimethyl-8-ribityllumazine (**3**) (2.5−200 μM) to a total volume of 1000 μL. The formation of riboflavin (**4**) was measured online with a computer-controlled photometer at 470 nm ($\epsilon_{riboflavin}$ = 9100 M^{-1} cm^{-1}). The K_i evaluation was performed in the same manner as described above.

Acknowledgment. This research was made possible by NIH Grant No. GM51469 as well as by support from the Deutsche Forschungsgemeinschaft and Fonds der Chemischen Industrie.

Supporting Information Available: Procedures and analytical data for the synthesis of compounds **29** and **30**. This material is available free of charge via the Internet at http://pubs.acs.org.

JO030278K

(30) Liao, D.-I.; Wawrzak, Z.; Calabrese, J. C.; Viitanen, P. V.; Jordan, D. B. *Structure* **2001**, *9*, 399−408.
(31) Kis, K.; Bacher, A. *J. Biol. Chem.* **1995**, *270*, 16788−16795.
(32) Kuzmic, P. *Anal. Biochem.* **1996**, *237*, 260−273.
(33) Eberhardt, S.; Richter, G.; Gimbel, W.; Werner, T.; Bacher, A. *Eur. J. Biochem.* **1996**, *242*, 712−718.